Pulse-induced alternation from bipolar resistive switching to unipolar resistive switching in the $Ag/AgO_x/Mg_{0.2}Zn_{0.8}O/Pt$ device

2012 J. Phys. D: Appl. Phys. 45 425303

(http://iopscience.iop.org/0022-3727/45/42/425303)

IOP PUBLISHING JOURNAL OF PHYSICS D: APPLIED PHYSICS

J. Phys. D: Appl. Phys. **45** (2012) 425303 (5pp) doi:10.1088/0022-3727/45/42/425303

Pulse-induced alternation from bipolar resistive switching to unipolar resistive switching in the Ag/AgO_x/$Mg_{0.2}Zn_{0.8}O$/Pt device

L L Wei[1,2], J Wang[1], Y S Chen[1], D S Shang[1], Z G Sun[2], B G Shen[1] and J R Sun[1]

[1] Beijing National Laboratory for Condensed Matter Physics and Institute of Physics, Chinese Academic of Sciences, Beijing 100190, People's Republic of China
[2] State Key Laboratory of Advanced Technology for Material Synthesis and Processing, Wuhan University of Technology, Wuhan 430070, People's Republic of China

E-mail: wangjing@iphy.ac.cn, yschen@iphy.ac.cn and jrsun@iphy.ac.cn

Received 31 May 2012, in final form 8 August 2012
Published 4 October 2012
Online at stacks.iop.org/JPhysD/45/425303

Abstract
Electric field-induced resistive switching (RS) and related effects are studied for the ZnO-based device Ag/AgO_x/$Mg_{0.2}Zn_{0.8}O$/Pt. The system exhibits a bipolar resistive switching (BRS) for the current (I)–voltage (V) cycles, with the set/reset voltage distributing in a narrow region around 0.15 V/0.16 V. The high to low resistance ratio is ∼10, and the resistive state is well retainable. However, the RS becomes unipolar (unipolar resistive switching—URS) when electric pulses are applied, with a fairly wide distribution of the set/reset voltages, though the resistive state is still well retainable. It was further found that a backward transition from the URS to the BRS state can be occasionally triggered by simply performing I–V cycling in the negative branch, which shows the strong competition of the BRS and URS states. Both the BRS and URS states were stable and reproducible over 90 cycles. Possible mechanisms for the BRS and URS state and their mutual transition were discussed.

(Some figures may appear in colour only in the online journal)

1. Introduction

Electric field-induced resistive switching (RS) in transition metal oxide films has attracted considerable attention due to its potential applications. The resistive random access memory (RRAM) designed based on this effect could be the next generation of nonvolatile memory technology, replacing the traditional one due to its simple structure, low power consumption, high operation speed and high integration density. Up to now, the RS effect has been reported in a wide variety of solid-state materials, including binary transition metal oxides [1–3], perovskite oxides [4–7] and organic materials [8]. According to whether the switching characteristic depends on electric polarity or not, the RS behaviour can be classified into two types: bipolar resistive switching (BRS) and unipolar resistive switching (URS). In the former case, the transition from the high resistive state (HRS) to the low resistive state (LRS) of the device (the set process) occurs at one electric polarity, whereas the reverse transition (the reset process) takes place under the opposite field. In contrast, the URS happens only above a threshold current, regardless of polarity. In general, there is only one switching type for a given RRAM device. The perovskite oxide-based devices, such as Cr-doped $SrZrO_3$ [6], Sr_2TiO_4 [4] and PCMO [5], often show a BRS, whereas the binary oxide-based devices, such as NiO [2], Cu_2O [9] and TiO_2 [1, 3], exhibit the URS or BRS, depending on the preparation condition of the sample. Different characteristics are observed for these two switching behaviours. The BRS features a higher switching speed, lower power consumption and better endurance than

the URS does, whereas the URS features a greater high to low resistance ratio [10, 11]. Hence it may expand the application scope in nonvolatile memories to develop devices that can reversibly transit between the BRS state and URS state. Recently, a signature for this has been observed in special materials/devices. By increasing the forming current, Jeong *et al* [12] successfully obtained a transition from the BRS to the URS for the Pt/TiO_2/Pt sandwich structure that is originally known as a BRS device. Following the same approaches as those of Jeong *et al*, Sun *et al* [13] and Shen *et al* [14] studied the reversible transition between the BRS and URS for the Au/$SrTiO_3$/Pt and Pt/BST/Pt devices, respectively. Here we report on a transition from the BRS to the URS state in the Ag/AgO_x/$Mg_{0.2}Zn_{0.8}O$/Pt device. Different from the previous works, this transition is triggered by electric pulses, instead of increasing forming current compliance. Meanwhile, by performing I–V cycling in the negative branch, a reverse transition from the URS to the BRS occurs. Under the impact of electric pulses, thin and imperfect conduction filaments could be formed across the device. In this case the effect of Joule heating may be important in a sense that it can cause a breakdown of weakly linked conductive fragments before the ion migration in electric field occurs, leading to the BRS to URS transition.

2. Experimental

The Mg doped ZnO ceramic target was obtained by mixing ZnO and MgO powders in the atomic ratio of Zn : Mg = 8 : 2, grinding and sintering the resultant mixture at 900 °C for 10 h in air. $Mg_{0.2}Zn_{0.8}O$ films, ~170 nm in thickness, were deposited on the Pt/Ti/SiO_2/Si substrates by the pulsed laser deposition technique. The temperature of the substrate is ~400 °C and the oxygen partial pressure is ~30 Pa. Above the $Mg_{0.2}Zn_{0.8}O$ film, a AgO_x buffer layer of the thickness of 20 nm was deposited using a silver target under an oxygen pressure of ~10 Pa at room temperature. After that, the chamber was evacuated to 5×10^{-4} Pa and then Ag discs of 0.2 mm diameter were deposited using a shadow mask, The whole thickness of the Ag/AgO_x layer is about 100 nm. As illustrated in the inset of figure 1, the Ag top electrode (TE), the AgO_x buffer layer, the $Mg_{0.2}Zn_{0.8}O$ matrix layer and the Pt bottom electrode (BE) constitute a metal–insulator–metal (MIM) RRAM device.

The crystal structure of the sample was characterized by x-ray diffraction (XRD, Rikagu diffractometer D/MAX-2500) with Cu Kα radiation. The resistance switching characteristics of the $Mg_{0.2}Zn_{0.8}O$-based RRAM cells were measured by a Keithley 2611 Source Meter. The positive polarity was defined as the direction from the TE to the BE. Voltage pulse was generated by an Agilent 33250A waveform generator and the response signals were captured by a Tektronix TDS 3052C digital phosphor oscilloscope. All the measurements were conducted at room temperature.

3. Results and discussion

Figure 1 shows the XRD pattern of the $Mg_{0.2}Zn_{0.8}O$ film on the Pt/Ti/SiO_2/Si substrate. Totally four diffraction peaks are

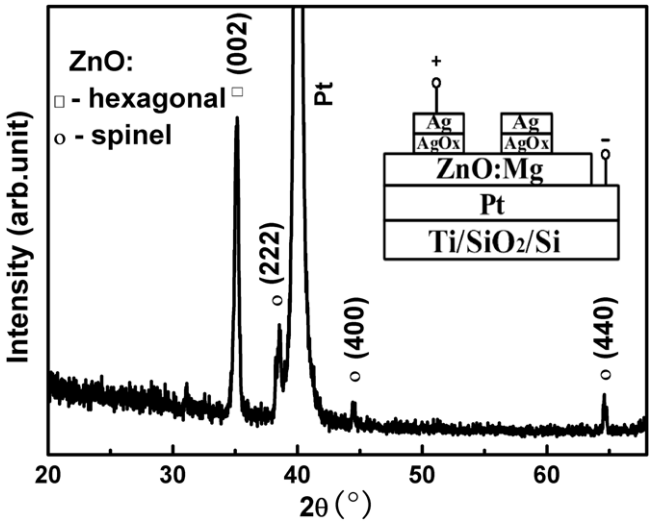

Figure 1. The XRD pattern of the $Mg_{0.2}Zn_{0.8}O$ film on the Pt/Ti/SiO_2/Si substrate. The inset is the schematic configuration of the Ag/AgO_x/$Mg_{0.2}Zn_{0.8}O$/Pt device.

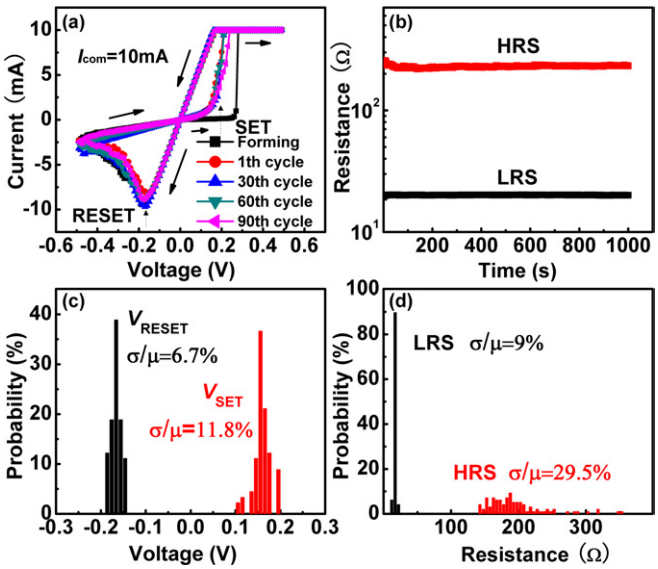

Figure 2. (*a*) Typical BRS characteristics of the Ag/AgO_x/$Mg_{0.2}Zn_{0.8}O$/Pt device with a current compliance of 10 mA, black square shows the forming process. (*b*) Retention characteristics of the LRS and HRS in the BRS device at room temperature. The resistance values were measured at 0.5 V. (*c*), (*d*) The statistical distributions of the programming voltages (V_{SET}, V_{RESET}) and the resistance values of LRS and HRS, respectively.

detected in the 2θ range 20°–65°, belonging to a hexagonal phase (0 0 2) and a spinel phase (2 2 2), (4 0 0) and (4 4 0), respectively. The former is the main phase and high textured, as indicated by the sharp and strong peak. This can be attributed to the low surface energy of the (0 0 2) plane and the small lattice mismatching (1.4%) between the c plane of the thin films and the Pt (1 1 1) plane [15]. The inset in figure 1 gives the schematic diagram of the sample.

Figure 2(*a*) shows the typical BRS behaviour of the Ag/AgO_x/$Mg_{0.2}Zn_{0.8}O$/Pt device measured by DC sweeps. The voltage was applied in the sequence of 0 → +0.5 → 0 → −0.5 → 0 V at a speed of 10 mV s^{-1}. The current

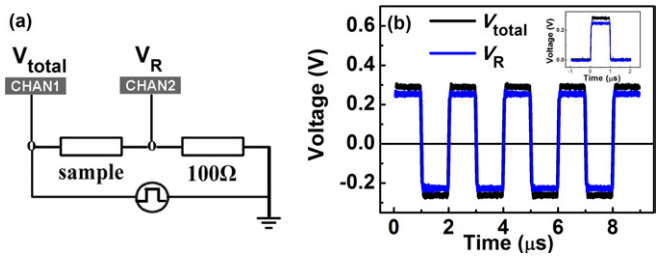

Figure 3. (*a*) The schematic configuration of the pulse trigger measurement system. A load resistor R with the value of 100 Ω was adopted in series to the device. (*b*) The effect of successive alternating negative and positive voltage pulses. The amplitude of the pulse is 0.3 V with the width of 1 μs. The inset plot in (*b*) shows the effect of a single positive electric pulse. The device transits from the original high resistance state to a low resistance state after a single pulse.

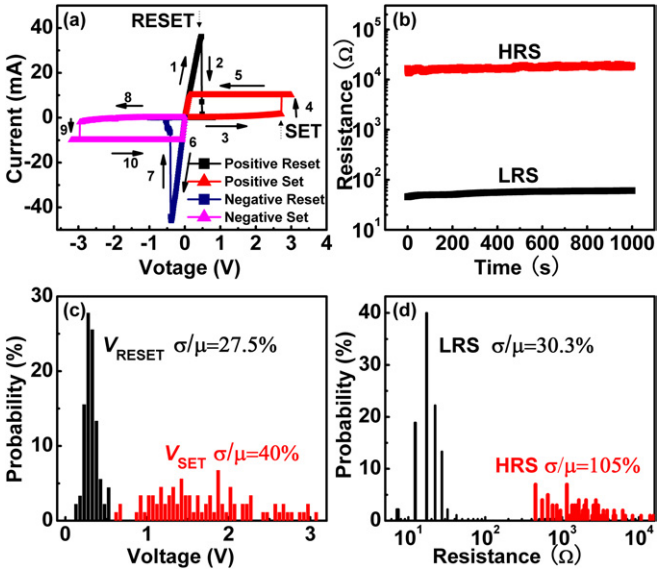

Figure 4. (*a*) Typical URS characteristics of the $Ag/AgO_x/Mg_{0.2}Zn_{0.8}O/Pt$ device with $I_{com} = 10$ mA. (*b*) Retention behaviour in the low- and high-resistance states, respectively, under the reading voltage of 0.5 V. (*c*), (*d*) The statistical distributions of the programming voltages (V_{SET}, V_{RESET}) and the resistance values of LRS and HRS, respectively.

compliance was set to $I_{com} = 10$ mA to obtain good switching performance. The pristine device exhibited an initial resistance of 1.6×10^3 Ω. In the forming process, when gradually increasing the positive applied voltage to $V_{Forming} = 0.26$ V, the current suddenly jump to I_{com}, indicating a transition to the LRS. The device remained in the LRS during the bias descending process, and an idealized linear I–V relation is observed. This Ohmic behaviour persists until the bias voltage swept to $V_{RESET} = -0.18$ V, where the device switched back to the HRS. After the forming process, repeatable BRS behaviour was observed, with the set voltage of $V_{SET} = 0.18$ V and reset voltage of $V_{RESET} = -0.18$ V. The overlap of 90 cycles of the I–V curves shows a good uniformity performance of the $Ag/AgO_x/Mg_{0.2}Zn_{0.8}O/Pt$ device.

Figure 2(*b*) shows the retention data of the HRS and LRS, collected under the reading voltage of 0.05 V. The high to low resistance ratio is $R_{HRS}/R_{LRS} \approx 10$, and no significant changes in resistance magnitudes are observed within 10^3 s for both the HRS and LRS. The latter clearly reveals the nonvolatile characteristics of the memory. As shown in figures 2(*c*) and (*d*), both the set/reset voltages and the resistance values of the HRS and LRS demonstrate narrow distributions. The V_{SET} varies from 0.11 to 0.19 V with the σ/μ value of 6.7% and the V_{RESET} vary from −0.14 to −0.18 V with the σ/μ value of 11.8%, where σ is the mean square error and μ is the mean value. Both the set and reset voltages are obviously lower than those in most reported RS devices [10, 16, 17], which is beneficial to the practical application of RRAM. Meanwhile, the LRS values range from 12 to 22 Ω with a σ/μ ratio of 9%. Different from the LRS, the resistance of the HRS distributes in a relatively wide range. After all, the experimental results of the BRS behaviour in the $Ag/AgO_x/Mg_{0.2}Zn_{0.8}O/Pt$ device exhibit good reliability.

The device was then linked in series to a standard resistor of 100 Ω. By measuring the voltage drop on the standard resistor while electric pulses were applying, the resistance of the device can be deduced. Figure 3(*a*) shows the schematic configuration of the pulse trigger measurement system. The switching pulse was generated by an Agilent 33250A waveform generator and the response signals were monitored by a Tektronix TDS 3052C oscilloscope through the in-series resistor. The resistance (R_{device}) of the device can be calculated based on the formula of $R_{device} = (V_{total} - V_R)/(V_R/100)$, where V_R is the voltage dropped on the load resistor and V_{total} is the output voltage of the generator. After the $Ag/AgO_x/Mg_{0.2}Zn_{0.8}O/Pt$ device was reset to the HRS by dc voltage sweeping, successive alternating positive and negative voltage pulses were then applied to the series circuit. The electric pulse is 0.3 V in amplitude and 1 μs in width. As shown in figure 3(*b*), V_{total} and V_R are ∼0.3 V and ∼0.25 V, respectively, and hardly change under the impact of successive pulses. A direct calculation leads to the device resistance of 20 Ω. This result indicates that the HRS of the device obtained from the dc reset process was already switched to LRS after the first positive pulse (the inset in figure 3(*b*)). The device remains in the LRS under the impact of subsequent pulses, regardless of pulse polarity.

After the treatment of electric pulses, fascinatingly, the device exhibited the I–V characteristics of the typical URS devices. As shown in figure 4(*a*), the current increases linearly with applied voltage until a threshold $V_{RESET} \approx 0.5$ V is reached. After that a sudden drop in current occurs, marking the LRS to HRS transition. When repeating the voltage sweeping without changing polarity, the device switched backwards to the LRS at a large set voltage of about 2.5 (current compliance 10 mA). The set and reset processes occurred symmetrically for the positive and negative voltage sweepings, a behaviour of the typical URS devices.

The retention measurement shown in figure 4(*b*) indicates that the HRS and LRS of the URS type are also nonvolatile. The high to low resistance ratio is over 100, much greater than that observed in the BRS mode. The V_{SET} and V_{RESET} values distribute in the range from 0.1 V to 0.5 V and from 0.6 V to 3 V, respectively (figure 4(*c*)). The resistance values

of the LRS range from 7 to 32 Ω, while the HRS from 450 to 15 kΩ (figure 4(*d*)). Compared with those in the BRS mode, the distributions of switching parameters in the URS mode, namely the switching voltage and resistance, are much wider. As shown in figure 4(*c*), the set voltage dispersed in the range from ∼1 to ∼3 V, indicating the randomness of the HRS to LRS transition. As well documented, the URS behaviour arises from the formation and rupture of conductive filaments, respectively, induced by electric field and Joule heating. The large distributions of the set and reset voltages and the HRS and LRS resistances reflect the inhomogeneity of the conductive filaments.

The above results clearly show the BRS to URS transition triggered by electric pulses in the Ag/AgO_x/$Mg_{0.2}Zn_{0.8}O$/Pt device. The current in the pulse testing is only 3 mA, which is less than the current compliance of bipolar mode (I_{com} = 10 mA). This means that, different from continuous dc electric field, electric pulses with smaller current compliance can lead to a bipolar to unipolar transition. This feature may be beneficial for the practical application of the corresponding devices.

Recently, by selecting a lower or higher current compliance for the forming process, Lee *et al* [18] found that the transport behaviour of the Ag/ZnO/Pt device can be either BRS or URS: The resistance of the LRS was driven to much lower values by increasing current compliance, and the *I*–*V* relation thus resulted becomes URS in character. It is argued that filaments will be coarse in diameter and dense in distribution under high forming currents, which is responsible for the URS behaviour of the device. We also studied the switching characteristics of the Ag/AgO_x/$Mg_{0.2}Zn_{0.8}O$/Pt devices with an increased current compliance, and no BRS–URS transition is observed even the compliance for the forming current is as high as 100 mA (the current density is ∼1.5 times as large as that used by Lee *et al*). Further increase in current compliance leads a breakdown of the sample. These results manifest the impossibility to realize the BRS–URS conversion simply by choosing large current compliances, thus the different mechanisms of the switching type transition in Ag/AgO_x/$Mg_{0.2}Zn_{0.8}O$/Pt.

It is worth noting that the URS behaviour of the Ag/AgO_x/$Mg_{0.2}Zn_{0.8}O$/Pt device could transit backwards to BRS through an appropriate measurement sequence. When a negative voltage was applied to the LRS of URS mode, two kinds of reset process would occur randomly. The main reset process is the URS behaviour as indicated in figure 4(*a*), resulting in a HRS with a resistance of about 10^3 Ω. In this case, the device remains the URS state. However, as shown in figure 5, there is also a reset process which leads to a HRS with a lower resistance (∼180 Ω). In this case, the device enters into the BRS state, as shown by the subsequent voltage sweeping along the route of 0 → +0.5 → 0 → −0.5 → 0 V (The current compliance is I_{com} = 10 mA, and the set and reset voltages are about 0.2 V and −0.16 V, respectively). The latter process occurs with a probability of about 10%. The experimental results show that the backward transition to the BRS is random in nature, which implies the occurrence of two competitive reset processes. As well

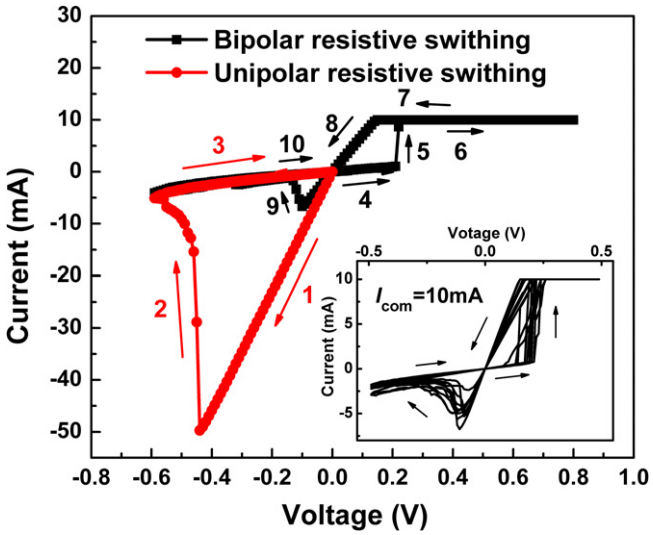

Figure 5. The device transited to BRS (black square) when negative voltage was applied to the LRS of USR mode (red diamond). Inset: BRS characteristics after transition.

known, there are two processes in the presence of an electric bias, i.e. the migration of Ag ions driving by electric field and the breakdown of conduction filaments by Joule heating. These two processes may occur simultaneously, and the one that is preponderant determines the nature of the resistance switching.

A simplified model based on the filament's formation and rupture is illustrated in figure 6, which can explain the mechanisms for the bipolar and unipolar switch. In the BRS mode, under positive biases the Ag^+ ions near the AgO_x/$Mg_{0.2}Zn_{0.8}O$ interface migrated from the TE towards the BE, and then reduced there. This in turn leads to the conductive filaments that stemmed from the BE and grew towards the TE, thus the HRS to LRS switching (figure 6(*a*)). The switching-off process achieved by the electrochemical dissolution of Ag atoms in the AgO_x-$Mg_{0.2}Zn_{0.8}O$ interface (figure 6(*b*)). This is similar to that occurred in the Ag/ZnO : Mn/Pt device, which exhibits BRS due to the formation and rupture of nanoscale Ag bridges in the ZnO : Mn films [19]. When the electric pulse that is several microseconds in width was applied, conductive filaments can also be formed. Considering the fact that the Ag^+ cation migration, reduction and arrangement complete in microseconds, the conductive path in LRS of the URS mode could be far from perfection. It may be formed by weakly linked fine channels, especially near the TE (figure 6(*c*)). In this case, applying a positive electric field again to the device would lead to a thermal dissolution of the thinner paths due to the strong Joule heating, thus the LRS to HRS switching of the URS mode (figure 6(*d*)).

Because of the positive feedback of thermal dissolution, the resistance of the HRS of the URS state is much higher than that of the BRS state. However, if a negative reset voltage was applied, two processes associated with the migration of the Ag^+ cations and the thermal dissolution of the Ag filaments will take place. As a consequence, either the BRS or the URS state can be resulted (figures 4(*a*) and

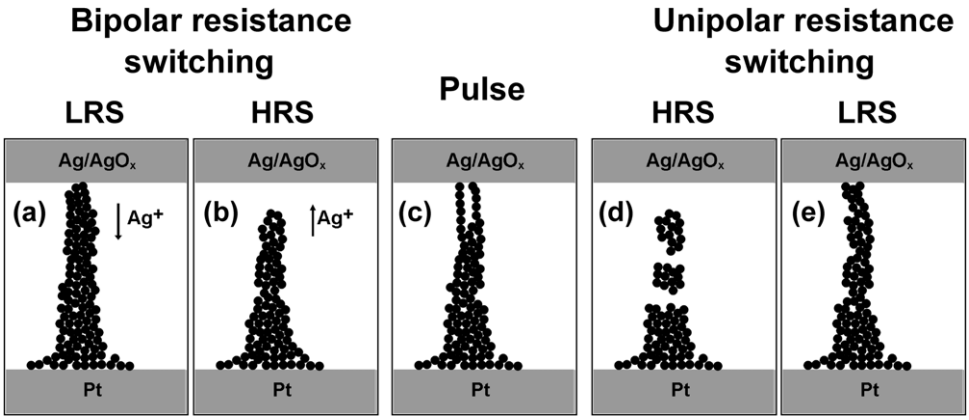

Figure 6. A simplified filament model for the explanations of the bipolar and the unipolar switching mechanisms. (*a*), (*b*) The device showed bipolar switching because the filament formed and dissolved due to the Ag^+ cation migration in electric field. (*c*) Thin and imperfect channels formed near the interface area after a pulse trigger. (*d*) Thinner parts of Ag CFs ruptured due to Joule heating origin from the local stress concentration. (*e*) Formation of CFs in the URS set process.

5), depending on the result of the competition of these two processes.

4. Conclusions

In this paper, we report the coexistence of BRS and URS in the $Ag/AgO_x/Mg_{0.2}Zn_{0.8}O/Pt$ device. The transport properties of the device in these two states have been investigated in detail. The device exhibits reliable BRS behaviour with a quite narrow threshold voltages distributions (V_{SET} = 0.11–0.19 V, V_{RESET} = −0.14 ∼ −0.18 V). The high-to-low resistance ratio is ∼10, and the resistive state is well retainable. However, the RS becomes unipolar (URS) when electric pulses are applied between successive *I*–*V* cycles, with a fairly wide distribution of the set/reset voltages, though the resistive state is still well retainable. It was further found that a backward transition from the URS to the BRS state can be occasionally triggered by simply performing the *I*–*V* cycling in the negative branch, which shows the strong competition of the BRS and URS states. Both the BRS and URS states were stable and reproducible over 90 cycles. A conductive filament model based on the competition of electrical bias caused ions migration and Joule heating induced thermal dissolution is introduced to explain the switching mechanisms and origin of switching mode transition.

Acknowledgments

This work has been supported by the National Basic Research of China, the National Natural Science Foundation of China, the Knowledge Innovation Project of the Chinese Academy of Sciences, the Beijing Municipal Natural Science Foundation.

References

[1] Choi B J *et al* 2005 *J. Appl. Phys.* **98** 033715
[2] Kim D C *et al* 2006 *Appl. Phys. Lett.* **88** 202102
[3] Jeong D S, Schroeder H and Waser R 2009 *Phys. Rev.* B **79** 195317
[4] Shibuya K, Dittmann R, Mi S and Waser R 2010 *Adv. Mater.* **22** 411
[5] Liu S Q, Wu N J and Ignatiev A 2000 *Appl. Phys. Lett.* **76** 2749
[6] Beck A, Bednorz J G, Gerber C, Rossel C and Widmer D 2000 *Appl. Phys. Lett.* **77** 139
[7] Shen W, Dittmann R, Breuer U and Waser R 2008 *Appl. Phys. Lett.* **93** 222102
[8] Song Y, Ling Q D, Lim S L, Teo E Y H, Tan Y P, Li L, Kang E T, Chan D S H and Zhu C 2007 *IEEE Electron Device Lett.* **28** 107
[9] Chen A, Haddad S, Wu Y C, Lan Z, Fang T N and Kaza S 2007 *Appl. Phys. Lett.* **91** 123517
[10] Xu N, Liu L F, Sun X, Chen C, Wang Y, Han D D, Liu X Y, Han R Q, Kang J F and Yu B 2008 *Semicond. Sci. Technol.* **23** 075019
[11] Schroeder H and Jeong D S 2007 *Microelectron. Eng.* **84** 1982
[12] Jeong D S, Schroeder H and Waser R 2007 *Electrochem. Solid-State Lett.* **10** G51
[13] Sun X W, Li G Q, Zhang X A, Ding L H and Zhang W F 2011 *J. Phys. D: Appl. Phys.* **44** 125404
[14] Shen W, Dittmann R and Waser R 2010 *J. Appl. Phys.* **107** 094506
[15] Chen X M, Wu G H and Bao D H 2008 *Appl. Phys. Lett.* **93** 093501
[16] Li M, Zhuge F, Zhu X J, Yin K B, Wang J Z, Liu Y W, He C L, Chen B and Li R W 2010 *Nanotechnology* **21** 425202
[17] Guoa X, Schindler C, Menzel S and Waser R 2007 *Appl. Phys. Lett.* **91** 133513
[18] Lee S, Kim H, Park J and Yonga K 2010 *J. Appl. Phys.* **108** 076101
[19] Yang Y C, Pan F, Liu Q, Liu M and Zeng F 2009 *Nano Lett.* **9** 1636